CORROSION SCIENCE AND TECHNOLOGY, Vol.9, No.2(2010), pp.98~103

Corrosion Behavior of a High-Manganese Austenitic Alloy in Pure Zinc Bath

Zhang Yi†, LIU Junyou, and WU Chunjing

School of Materials Science and Engineering, University of Science and Technology, Beijing
(Received July 27, 2009; Revised April 7, 2010; Accepted April 8, 2010)

In order to further reduce the cost without reducing the corrosion resistance,a high-manganese austenitic alloy for sink roll or stabilizer roll in continuous hot-dip coating lines was developed. A systematic study of corrosion behavior of the high-manganese austenitic alloy in pure zinc bath at 490 ℃ was carried out. The results shows that, the high-manganese austenitic alloy shows better corrosion resistance than 316L steel. The corrosion rate of the high-manganese austenitic alloy in pure zinc bath is calculated to be approximately 6.42×10^{-4} g · cm^{-2} · h^{-1}, while the 316L is 1.54×10^{-3} g · cm^{-2} · h^{-1}. The high-manganese austenitic alloy forms a three-phase intermetallic compound layer morphology containing Γ, δ and ζ phases, while the 316L is almost ζ phase. The Γand δ phases of the high-manganese austenitic alloy contain about 8.5 wt% Cr, the existence of Cr improve the stabilization of phases, which slow down the reaction of Fe and Zn, improve the corrosion resistance of the high-manganese austenitic alloy. So substitute the nickel with the manganese to manufacture the high-manganese austenitic alloy of low cost is feasible.

Keywords *: corrosion, hot-dip coating, zinc bath, high-manganese alloy*

1. Introduction

Hot-dip galvanizing is of vital importance as it is the most effective and most popular method of corrosion protection for iron.[1)] In continuous hot-dip coating lines, the immersed bath hardware (e.g. submerged roll, stabilized roll and bearings) is subject to corrosive attack by the pure zinc bath. It is severely holdback the further development of the hot-dip industry.[2)] 316L stainless steel is the most popular and typical material for stabilizer and sink rolls in the industry.[3)] Due to 316L stainless steel contain quite a bit Ni and Mo, which improve the cost of hot-dip galvanized steel strip. Recent years, many researches is to found other potential materials for bath hardware instead of 316L stainless steel.[4)] After a series of researches, we developed a high-manganese austenitic alloy of low cost and good corrosion resistance. In this article, the corrosion behaviors of high-manganese austenitic alloy and the 316L stainless steel were studied and the mechanism of corrosion are discussed.

† Corresponding author: zhangyi198351@yahoo.com.cn

2. Experimental materials and methods

The induction melting of high-purity, raw materials was performed. The test specimens have dimensions of 15 mm x 10 mm x 5 mm. The specimens of High-manganese austenitic alloy and 316L stainless steel were immersed in 490 ℃ pure zinc bath for times of 1, 3, 5, 10 and 14 days. The specimens were cleaned and measured before immersion to the pure zinc bath. At the end of the testing time, the test specimens were removed from the zinc and measured again. The average thickness loss was used to calculate corrosion rate. The formula used to calculate the corrosion rate of the tested alloy is given below:[5)]

$$dw/dt = \rho \cdot (dy/dt) \cdot (1/2) \quad (1)$$

where dw/dt is corrosion rate g/cm^2 · h; ρ is density of base material, g/cm^3; dy/dt is average thickness loss per hour, cm/h. The factor of (1/2) in equation is used to reflect the fact that the average thickness change of the specimen is caused by the corrosion of both faces of specimen.

The microstructure and composition of the corrosion layer formed during the corrosion testing were successfully examined with the aid of INCA-300 optical microscopes and LEO-1450 scanning electron microscope. Thickness

measurements were taken with the aid of LEICA VMHT-30 microhardness instrument. Phase analysis was performed by D/MAX-RB X-ray diffraction technique.

3. Results

3.1 Microstructure of base materials

Optical micrograph and XRD analysis of high-manganese austenitic alloy can be seen in Fig. 1. According to the Fig. 1(a), the average grain size of the alloy is approximately 30 μm. There are some carbides and nitrides distributing in grain boundary. From Fig. 1(b), The alloy has absolutely austenite structure.

3.2 Corrosion rate

Relationship between thickness loss and corrosion time on the two specimens are shown Fig. 2. From this graph, for the two alloys, there are parabolic relationship of thickness loss over time with 316L exhibiting a greater thickness depletion than high-manganese austenitic alloy. Each parabolic trend line possess an initial high corrosion region then reach a quasi-steady state, where there is little change in the thickness of the reaction layer with test time. The

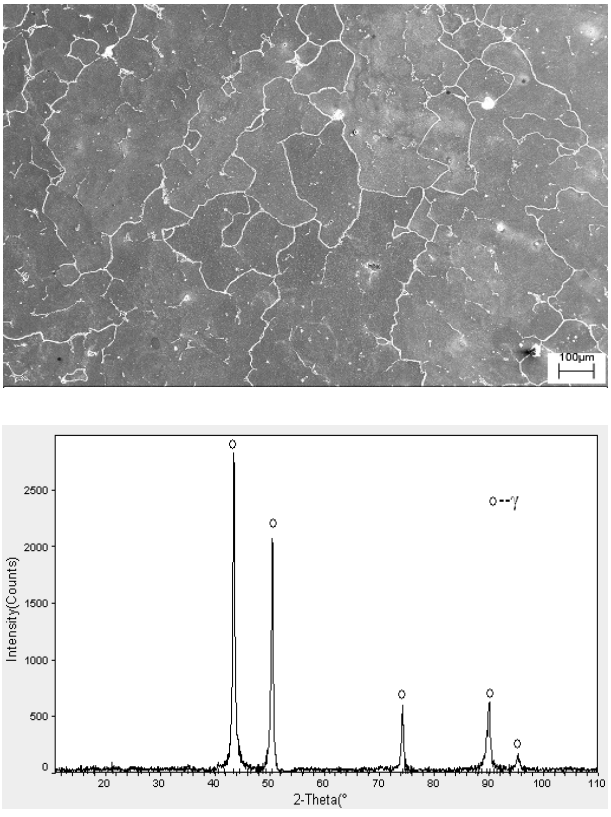

Fig. 1. SEM and XRD analysis of specimen used for corrosion testing.

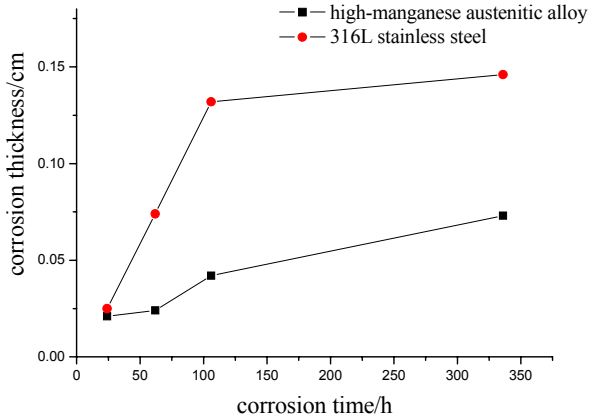

Fig. 2. Thickness loss of the two specimens in pure zinc bath.

thickness loss of the specimens can be observed to increase linearly with an increase in testing time before 100 hours, then the thickness has little change. In the whole corrosion time, the corrosion rate of high-manganese austenitic alloy and 316L stainless steel were approximately 6.42×10^{-4} g/cm2 · hr and 1.54×10^{-3} g/cm^2 · hr, respectively. So the high-manganese austenitic alloy shows better corrosion resistance than 316L stainless in the pure zinc bath.

2.3 Observation of the corrosion layer

Fig. 3 shows the optical and high magnified SEM micrographs of the high-manganese austenitic alloy dipping in pure zinc bath for different times. The EDS analysis of intermetallic products are displayed in Table 1. As seen in Fig. 3(a), after dipping in pure zinc bath for 1 day, the area on the right of the micrograph is the high-manganese austenitic alloy base material. To the left of the matrix, a thin alloy layer was observed. This intermetallic layer was approximately 20 μm in thickness and had a uniform and continuous structure. According to Fig. 3(b), with the increase of corrosion time, the reaction layer become much thicker and the Γ phase can be gathered by EDS. The first layer is Γ phase with an average composition of 7.59 wt% Cr, 0.30 wt%Mn, 12.29 wt% Fe, 1.01 wt%Si, 0.23 wt%Ni and 78.8 wt%Zn, the second is δ phase, which has an average composition of 6.88 wt% Cr, 7.95 wt% Fe, 0.61 wt%Si, 0.27 wt%Ni and 84.16 wt%Zn; the third is ζ phase, which has cylindrical structure and an average composition of 0.76 wt% Cr, 5.88 wt% Fe, 0.15 wt%Si and 92.96 wt%Zn. When dipping in zinc bath for 5 days, there are some crack in the layer of Γ phase, whose composition of 8.48 wt% Cr, 11.15 wt% Fe, 0.49 wt%Ni and 78.49 wt%Zn. The concentration of Cr in δ phase is also up to 8.96 wt%.

Fig. 4 shows the micrographs of high-manganese austenitic alloy and 316L stainless steel from pure zinc bath

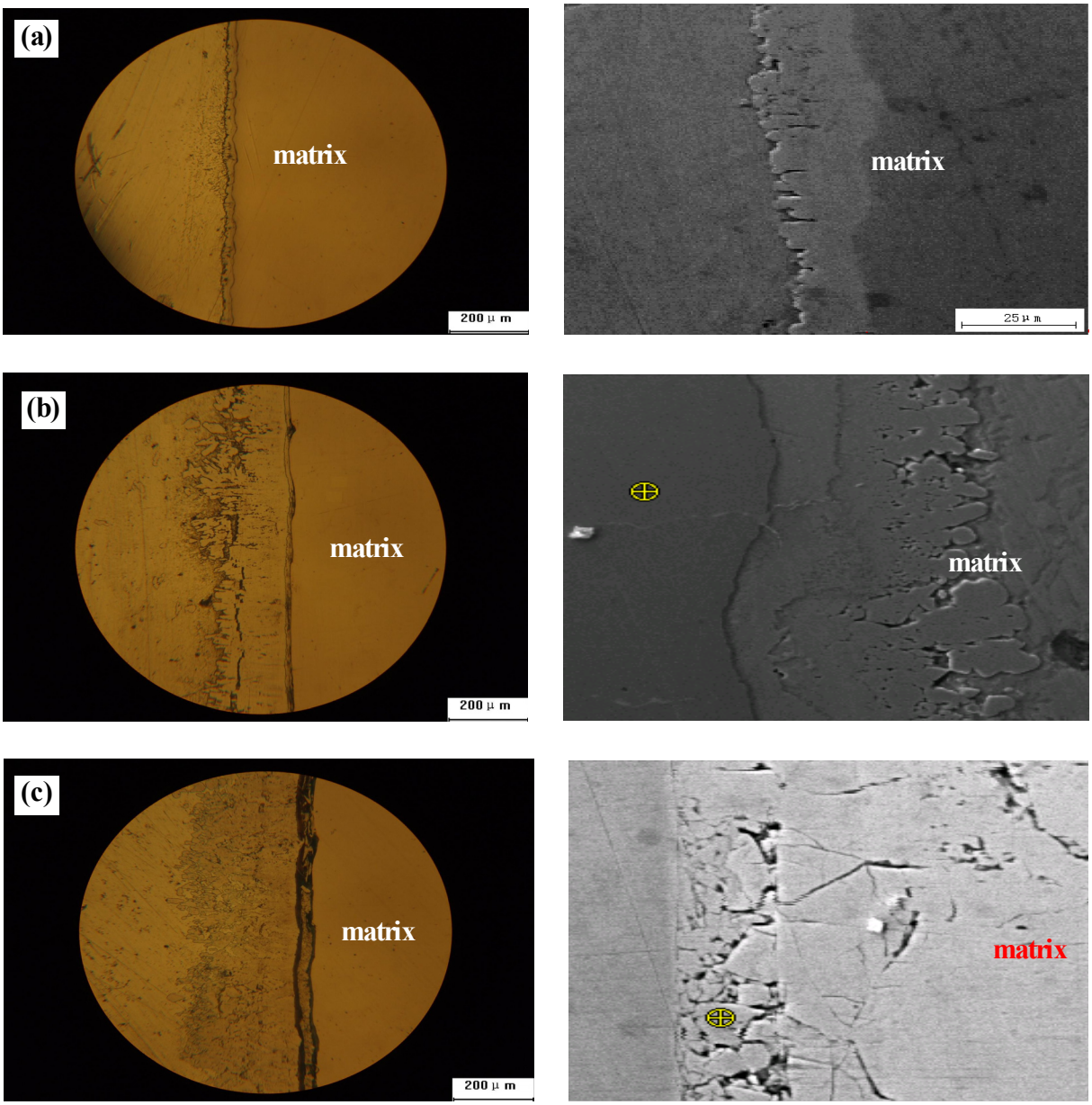

Fig. 3. Optical and high magnified SEM micrographs of high-manganese austenitic alloy dipping in pure zinc bath for different time: (a)1 day ; (b)3 days; (c)5 days.

for 14 days. The corrosion layer of high-manganese austenitic alloy forms a three-phase alloy layer morphology containing Γ, δand ζ phases and the layers of Γand δ phases are thin, while the ζ phase are very thick. There are a flat interface between matrix and corrosion layer. There are rough interface between 316L matrix and the corrosion layer for non-uniform corrosion happened, meanwhile The concentration of Cr in all intermetallic compound was less than 1% and the corrosion layer of 316L forms a one-phase alloy layer only containing ζ phase.

Fig. 5 shows line scan analysis across the intermetllic layer formed on steel specimens in pure zinc for 14 days. Across matrix to corrosion layer, the concentration of Fe, Zn, Cr and Mn changes sharply at interface. The concentration of Fe and Mn decreased sharply and that of Zn increased sharply. Mn had low concentration in whole corrosion layer, presumably the Mn was priority dissolved .There was little zinc in matrix but high concentration in whole corrosion layer.

There are high Cr concentration in Γ and δ layers, while little concentration in ζ layer. For the enrichment of Cr in corrosion layer, it exhibited dark colour .while other

Table 1. EDS anaylsis of intermetallic products formed on high-manganese austenitic alloy according to Fig. 3

Time	Position	Cr/wt%	Mn/wt%	Fe/wt%	Si/wt%	Ni/wt%	Zn/wt%	Phase composition
1 day	layer 1	5.43	-	6.30	-	-	88.10	δ phase
	layer 2	0.28	-	4.88	-	-	94.81	ζ phase
3 days	layer 1	7.59	0.30	12.29	1.01	0.23	78.8	Γ phase
	layer 2	6.88	-	7.95	0.61	0.27	84.16	δ phase
	layer 3	0.76	-	5.88	0.15	-	92.96	ζ phase
5 days	layer 1	8.48	-	11.15	-	0.49	78.49	Γ phase
	layer 2	8.96	0.20	6.74	1.06	-	82.83	δ phase
	layer 3	0.86	-	5.74	1.27	-	93.41	ζ phase

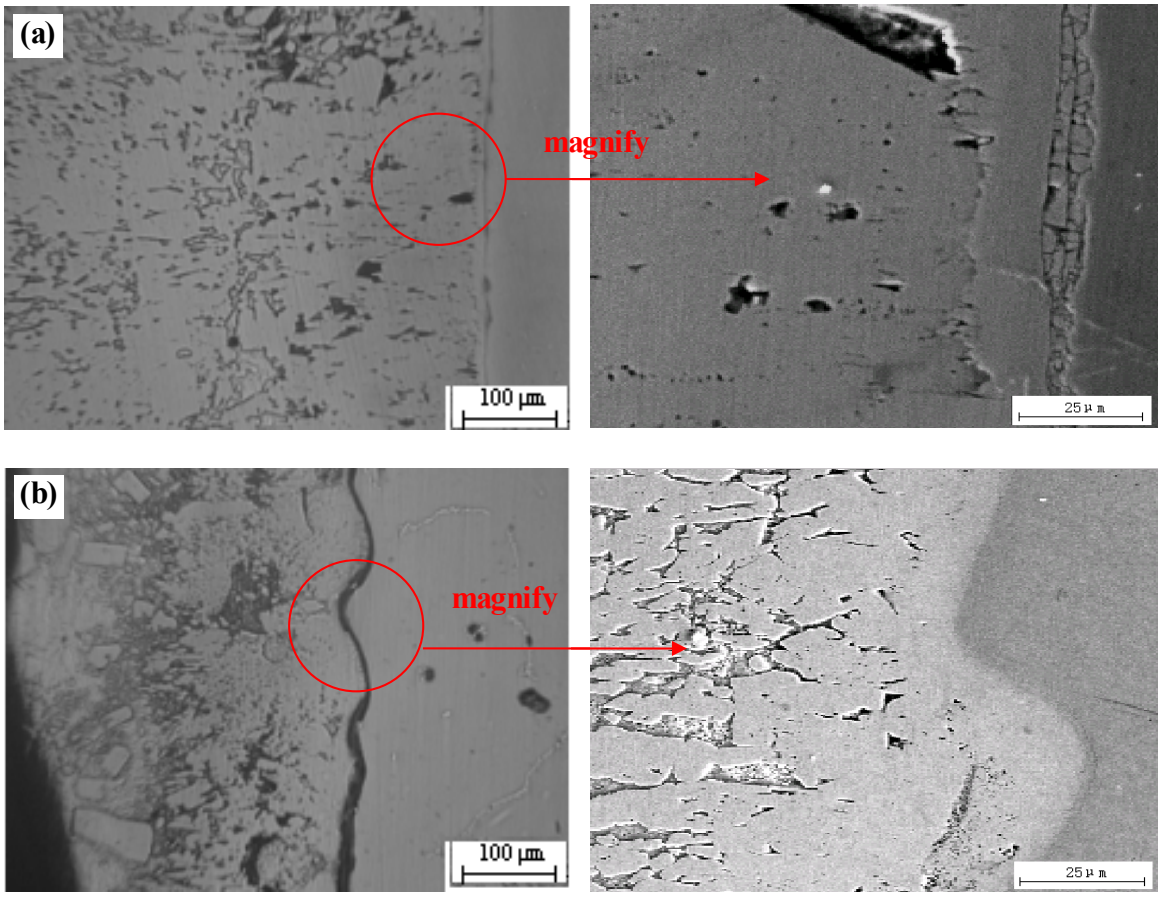

Fig. 4. Microstructure of two alloys dipping 14 days at 450℃ in Zn bath: high-manganese austenitic alloy (b)316L alloy.

regions with little Cr exhibited bright colour.

There are some crack in Γ phase, so it is easy to separate corrosion layer from matrix. Fig. 6 shows XRD pattern of the high-manganese austenitic alloy from pure zinc bath for 14 days. The corrosion products is Γ phase ($Fe_{11}Zn_{40}$), δ phase ($FeZn_{6.67}$, $FeZn_{8.87}$, $FeZn_{10.98}$), $Fe_4Mn_7Si_{19}$, $Mn_{22.6}Si_{5.4}C_4$, Mn, Cr_3Si and so on. The Cr element was not found in corrosion layer, presumably lots of Cr solid solution in Γ and δ phases.

4. Discussion

In pure Zn bath, the dominant corrosion reaction between the bath and the alloys is Fe from the alloys reacting with Zn to form a series Fe-Zn intermetallic compounds. The growth of the Fe-Zn phase was controlled by the dom-

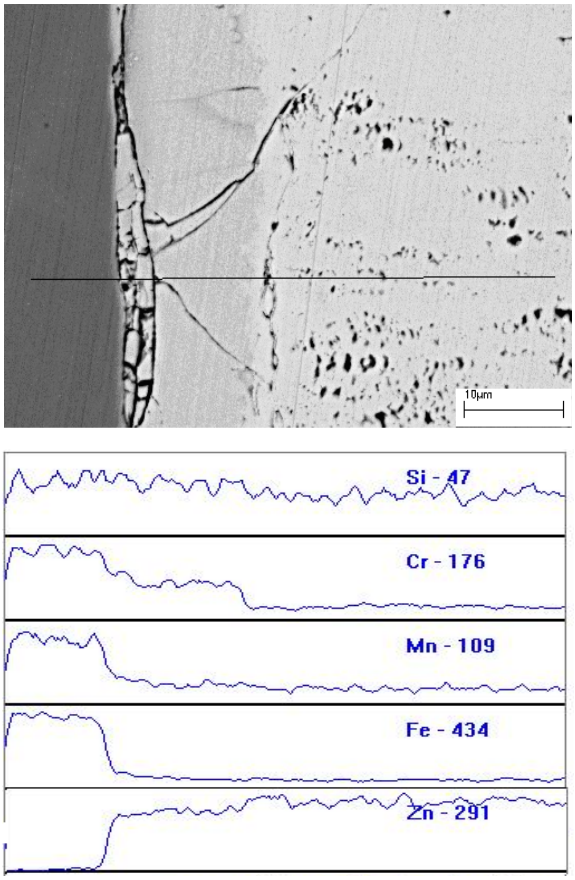

Fig. 5. Line scanning position and distribution of elements of the high-manganese austenitic alloy after dipping in a pure zinc for 14 days.

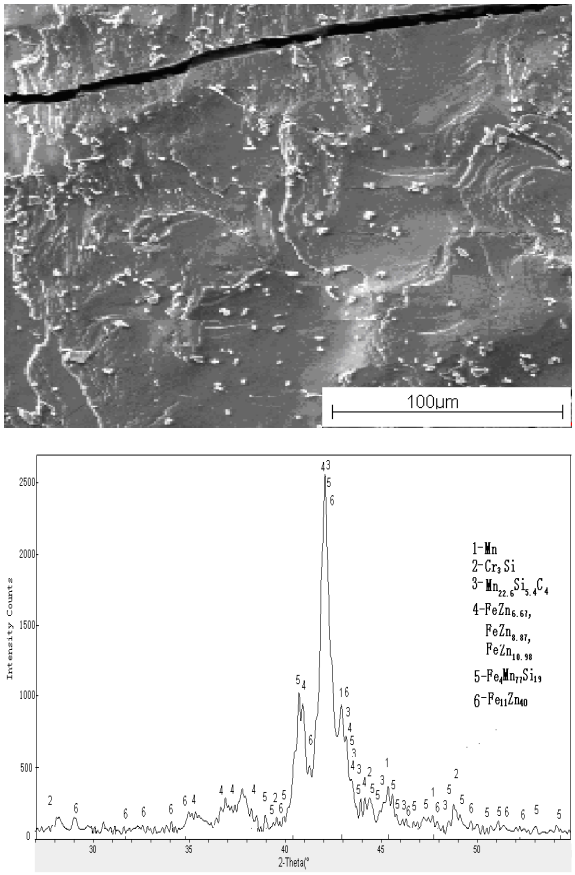

Fig. 6. XRD pattern of the austenite alloy with high Mn content after dipping in a pure zinc for 14 days.

inant one-sided diffusion of Zn through the phase layers toward the substrate Fe.[6),7)] the diffusion coefficient of zinc is greater than that for steel ($D_{Zn} > D_{Fe}$).[8)] Hence, it is widely believed that zinc readily diffuses intothe steel and forms intermetallic compounds. Dissolution mechanisms on steel by liquid zinc have been studied previously by several investigators.[9)-13)] According to the Fe-Zn binary phase diagram.[14)] There are some intermetallic compounds such as α, γ, Γ, Γ_1, δ, ζ and η phases. Firstly, α-Fe solid solution contain some zinc formed, then ζ phase is formed for its lowest heat of formation in all Fe-Zn intermetallic compounds. As the interdiffusion of Fe and Zn, the δ phase and Γ phase are subsequently formed.

The formation of Fe-Zn intermetallic compounds is divided two step: the first is combination reaction at interface; the second is the interdiffusion of Fe and Zn through existed Fe-Zn intermetallic compounds. Generally, the reaction of interface is more active than diffusion. The grow speed of the whole corrosion layer depend on two sides, one is diffusion velocity of Fe atom from matrix, the other is diffusion velocity of Zn atom through ζ and Γ phase. For different diffusion velocity of zinc in every phase, each phase layer has different thickness.

When the high-manganese austenitic alloy is dipped into pure zinc bath, the ζ phase is formed as the first Fe-Zn intermetallic compounds. Accompanied by interdiffusion of Fe and Zn ,the Fe-Zn phase continuously grow and the loose ζ phase near pure zinc bath is dissolved. The corrosion rate of the high-manganese austenitic alloy is decided by stabilization of the Fe-Zn phase. In other words ,the more stabilization of the Fe-Zn phases, the more corrosion resistance of the alloy. Alloy additions in steel (C, Si, Mn, Cr and so on) effect the interaction of Fe-Zn. The reaction of the steel with additions and Zn is no longer a simple binary system. The corrosion products must be ascertained by ternary or quaternary phase diagrams.

The existence of alloy addition with the high-manganese austenitic alloy, which effect the growth and stabilization of Fe-Zn intermetallic compounds. The corrosion resistance of high-manganese austenitic alloy is better than 316L stainless steel. For high-manganese austenitic alloy

has two aspects: the one is the formation of Γ phase contain many elements after corrosion for long time, For Γ phase and α-Fe phase have same crystal structure of bcc, They have adhesive each other. Once the formation of Γ phase, it reduce the process of diffusion and the corrosion rate ; the other is compact δ phase contain about 8.5% Cr, the existence of the Cr make the δ phase more stabilization .This δ phase act as a barrier reducing the reaction of Fe-Zn, at the same time improve corrosion resistance of the high-manganese austenitic alloy.

When 316L stainless steel dipping in pure zinc bath, the corrosion produces only contain ζ and δ phases with less than 1.5%Cr, with the increase of corrosion time, the Cr content of δ phase decrease, the stabilization of δ phase also reduce. After 14 days, the corrosion produce is almost ζ phase. The absence of Γ and δ phases increase the speed of Fe-Zn phases, so the 316L stainless steel.has a bad corrosion resistance.

Compare the high-manganese austenitic ally to 316L stainless steel, it would appear that the addition of Mn to an iron base produces a substantial increase in corrosion resistance, however, the addition of Ni to steel causes a significant deterioration in corrosion resistance, but at this stage of investigation it is difficult to put forward an explanation for the significant effect of Mn. On the other hand, the detrimental effect of Ni might well be associated with the affinity between Ni and Zn in forming intermetallic compounds.[15)]

5. Conclusions

1) The High-manganese austenitic alloy possessed better corrosion resistance than 316L stainless steel in pure zinc bath for 14 days, The corrosion rate of this two alloys were calculated to be approximately 6.42×10^{-4} g/cm^2 · h.and 1.54×10^{-3} g/cm^2 · hr respectively.

2) For dipping in pure zinc bath long time, the corrosion products of the High-manganese austenitic alloy is Γ, δ and ζ phases, while 316L stainless steel is almost ζ phase.

3) The high-manganese austenitic alloy had good corrosion resistance is for the existence of compact δ phase contain about 8.5% Cr, this δ phase act as a barrier reducing the reaction of Fe and Zn.

References

1. X. L. Ma, School of Materials Science and Engineering Shenyang University of Technology, Shengyang, **3**, 1 (2006) (in Chinese).
2. B. J. Wang, School of Materials Science and Engineering Beijing University of Technology, Beijing, **3**, 1 (2006) (in Chinese).
3. B. J Wang, W. J. Wang, and J. P. Lin, *Angang Technology*, **1**, 15 (2006) (in Chinese).
4. M.S. Brunnock, R.D. Jones, G.A. Jenkins, and D. T. Llewellyn. Ironmaking and Steelmaking, **23**, 171 (1996).
5. L. B. Matthew, West Virginia University, Master of Science in Mechanical Engineering, 27 (2000).
6. L. Xinbo, B. Ever, and J. Xu, *Metall. Mater. Trans. A*, **36**, 2049 (2005).
7. M. Onishi, Y. Wakamatsu, and H. Miura., *J. Inst. Met.*, **37**, 1279 (1973).
8. C. Allen and J. Mackowiak, *J. Inst. Met.*, **63**, 369 (1962).
9. A. R. Marder, *Prog. Mater. Sci.*, **45**, 191 (2000).
10. J. Mackowiak and N. R. Short, *Inter. Met. Rev.*, 1 (1979).
11. X. Liu, E. Barbero, and C. Irwin., AISTech 2005, Proceedings of the Iron & Steel Technology Conference, p. 403, Charlotte, North Carolina, U.S.A (2005)
12. G. Reumonta, J. B. Vogta, Iost, and J. Foct., *Surf. Coat. Tech.*, **139**, 265 (2001).
13. B. Peng, J. H. Wang, X. P. Su, Z. Li, and F. C. Yin, *Surf. Coat. Tech.*, **7**, 1 (2007).
14. A. Turnbull, M. W. Carroll, and D. H. Ferriss, *Corros. Sci.*, **30**, 667 (1990).
15. M. Andreani, P. Azou, and P. Bastien, C. R. Acad. Sci. Paris, **263**, 1041 (1966).